

Eurasian Chemical Communications

## Evaluation of C<sub>60</sub> nano-structure performance as nano-carriers of procarbazine anti-cancer drug using density functional theory methods

Behnam Farhang Rik<sup>a</sup>, Roya Ranjineh khojasteh<sup>a</sup>, Roya Ahmadi<sup>b,\*</sup>, Maryam Karegar Razi<sup>a</sup>

<sup>a</sup>Department of Inorganic Chemistry, Faculty of Chemistry, Tehran North Branch, Islamic Azad University, Tehran, Iran

<sup>b</sup>Department of Chemistry, Yadegar-e-Imam Khomeini (RAH) Shahre-rey Branch, Islamic Azad University, Tehran, Iran

Received: 3 January 2019, Accepted: 20 February 2019, Published: 1 July 2019

### Abstract

The study examined surface adsorption of fullerene C<sub>60</sub> with anticancer drug procarbazine in gas and solvent (water) phases using the DFT method. In doing so, the structure of the procarbazine, fullerene and their derivatives were first geometrically optimized in three different configurations with a base set of 6-31 g \* and B3LYP hybrid functions. Then, IR calculations, frontier molecular orbital, and molecular-based orbital analysis studies were performed on them. Additionally, thermodynamic parameters calculated including Gibbs free energy variation ( $\Delta G_{ad}$ ), erythrocyte formation ( $\Delta H_{ad}$ ) and thermodynamic properties (K) indicated that the reaction of procarbazine with fullerene C<sub>60</sub> is thermal, spontaneous, one-way and non-equilibrium. The effect of temperature on this substituent reaction was also examined and the results proved that at the temperature 314.15 K, the formation process would be best. The results of the computations showed that the results of the analysis of molecular orbitals indicate that the reactivity, electrophilicity, and conductivity of procarbazine are reduced after the substituent reaction. Computational examination of surface adsorption of procarbazine and fullerene C<sub>60</sub> nanostructures anticancer drugs using density functional theory (DFT) method.

**Keywords:** Procarbazine; anticancer drug; DFT; fullerene C<sub>60</sub>; drug deliver.

### Introduction

The rapid advance in drug discovery methods has led to an exponential increase in new drugs. Due to the diverse physicochemical properties of various drugs, we need smarter drug delivery systems. Among the critical issues in the pharmaceutical industry is the

discussion of controlled delivery of medicines to the body. With the common methods of medication administration such as oral and intestinal administration, the medicine will be distributed throughout the body and the whole body will be affected and the side effects of the drug will occur. In order to

\*Corresponding author: Roya Ahmadi

Tel: +98 (912) 2976055, Fax: +98 (21) 33810305

E-mail: roya\_ahmadi\_chem@yahoo.com

reach a particular effect, it is necessary to consume large amounts of the drug [1-4]. With nanotechnology, one can reach the targeted drug delivery and control the time, place and speed of drug release. New drug delivery systems have fewer side effects, more efficacies and more satisfaction and comfort for the patient [5-7]. Various carriers act as drug carriers in drug delivery. For ensuring the drug having a therapeutic effect, it must be protected in the body until reaching the target site. As the chemical and biological properties of some drugs are highly toxic and can have negative side effects, and if they are dissolved while releasing, their therapeutic effect decreases, and increasing the scope of bioavailability is rarely easily achieved by increasing the value of the drugs used [8]. For example, in chemotherapy, consumable drugs are toxic to some extent, and increasing them can have a reverse effect and even lead to death. In other words, if the medication can directly reach the target's position and is treated without any effect on other parts of the body, it is much better. Nanotechnology is very effective in developing new materials for increasing the bioavailability of drug delivery. In designing and developing carriers of drug delivery systems, the goal is to reach a system with appropriate loading of the drug and desired desirable liberation properties with a high half-life and low toxicity. Among the carriers used in drug delivery, fullerene can be cited. The

chemical structure of procarbazine is given in Fig. 1, and is used as an anticancer drug in chemotherapy [9-13]. Two categories of compounds recently considered a lot in the drug delivery are carbon nanotubes and fullerenes. Their size, shape and surface properties have made them available for use in drug delivery. Single-carbon nanotubes and 60 carbon fullerene have a diameter of about 1 nanometer, which is half the diameter of a DNA helix. Given their small size, these particles can easily pass through the width of membranes and biological barriers and get themselves into the cell. These structures can provide surface engineering at a high level. The surface of these particles is made loaded for increasing the solubility and biocompatibility, as well as the conductivity of different materials, with various groups and compounds. These particles can be used as carriers to carry biological molecules such as proteins, DNA and drugs [14-17]. Pharmaceutical compounds are loaded onto or within these structures. Making targeted and simultaneous transfer of two or more of the other components are of the other interesting characteristics of this particle in drug delivery. In this study, we try to evaluate and compute different nanostructures as nano-carriers of drugs from various aspects in the computer environment. The study examined the effect of fullerene C<sub>60</sub> the substituent on the energetic properties of procarbazine was first evaluated in a computational manner.

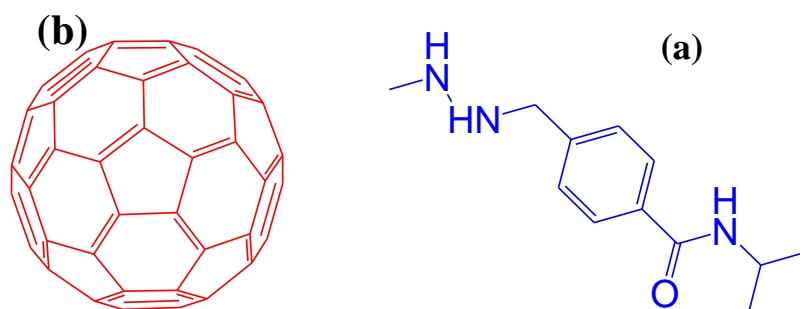
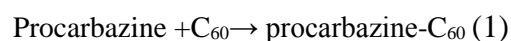


**Figure 1.** Chemical structure of procarbazine (a) and fullerene C<sub>60</sub> cage structure (b)

### Computational methods

Firstly, the structure of the procarbazine, fullerene C<sub>60</sub>, and the derivatives of the cited nanostructure reaction with the procarbazine were computed in three different modes using Gauss View 6.1 and Spartan software. In the next step, geometric optimization calculations, IR and molecular orbitals on them were performed using DFT and base series 6-31g\* with hybrid B3LYP functions. This basic series was selected as in previous reports the results of that match were in good agreement with experimental data. All calculations were performed using Spartan software in the temperature range from 278.15 to 314.15 K over the temperature range from 3°-3°. The reactions are examined in general using Equation (1)



Calculating and analyzing the value of enthalpy changes, the formation of the fullerene C<sub>60</sub> reaction with procarbazine was used to derive the amount of enthalpy formation for the fermentation process C<sub>60</sub> from the Equation (2). In this equation, ΔH<sup>0</sup> is the total energy variation in the process obtained by the reduction in the total energy of the products of a reaction from the sum of the total energy of the raw material. ΔH<sup>0</sup> also represents the enthalpy sign for each of the reaction components [18].

$$\Delta H_{\text{ad}} = E_{\text{C}_{60}\text{-Procarbazine}} - (E_{\text{C}_{60}} + E_{\text{Procarbazine}}) \quad (2)$$

Equation (3) was used to calculate the Gibbs free energy variation (ΔG<sub>ad</sub>). Regarding this, G<sub>th</sub> is the thermal

energy released by the Gibbs calculated by the software for each component of the reaction. The results, all of which are presented in Table (3), show that substituent of carbon nanotubes on procarbazine are spontaneous. This is because its ΔG<sub>ad</sub> is much less than the Gibbs III-Isomer free energy variation. It is noteworthy that the process of forming both derivatives is significantly more volatile by replacing the procarbazine at the fullerene bonding site. Since ΔG<sub>ad</sub> value has experienced a sharp decrease after the process. However, in general, as the value of this parameter is significantly negative in all cases, it can be expected that the reaction of forming all compounds is empirically possible. The effect of temperature on this quantity was also evaluated as is evident the temperature rises, the amount of Gibbs free energy changes gradually increases as well. Thus, the highest efficiency appears at room temperature or 278.15K Kelvin.

$$\Delta G_{\text{ad}} = E_{\text{C}_{60}\text{-Procarbazine}} - (E_{\text{C}_{60}} + E_{\text{Procarbazine}}) \quad (3)$$

The constant thermodynamic formation of the synthesis of procarbazine derivatives with fullerene was also calculated using Equation (4). In this equation, ΔG<sub>ad</sub> is the same as the Gibbs free energy variation obtained at the previous stage, R is the ideal gas constant, and T is the temperature in Kelvin as the results presented in Table (4) clearly show [19].

$$K_{\text{th}} = \exp(-\Delta G_{\text{ad}} / \quad (4)$$

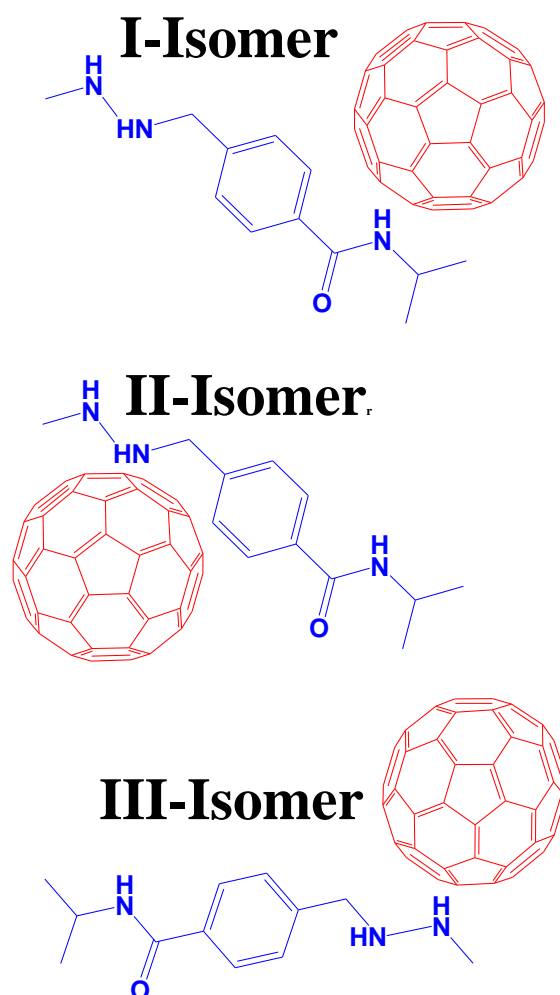


**Figure 2.** Optimized structure of procarbazine and its derivatives with fullerene  $C_{60}$

### Results and discussions

As seen in Figure 2, it approaches fullerene  $C_{60}$  from three situations. To understand more easily, each derivative of the procarbazine derivate with fullerene  $C_{60}$  is named with an abbreviation, which will be explained, the procarbazine is approaching the three positions (NH) to the  $C_{60}$  fullerene. The links between nitrogen atoms as well as the links between nitro groups and carbon and nitrogen atoms in the structure of procarbazine can play a key role in the effectiveness of synthesized. Procarbazine. In other words, as these links are looser and easier to disassociate, procarbazine can react more easily. Thus, after geometric

optimization was performed on all compounds, the length of C-NH bonds, in the pure procarbazine, as well as their derivatives with fullerene was measured and the values obtained in Table 1. As the data in Tables 1 indicate, after NH attachment to fullerene, the length of the bonds and N-C bonds have increased, meaning that these bonds become looser and these derivatives can more easily enter the process of effectiveness. Density is another parameter that has a direct and special relationship with effective power [20]. As is seen in the data in the tables, the procarbazine density has decreased after the connection to the pure fullerene  $F_{60}$ . Other structural features, such as surface

and zero-point energy have also increased dramatically after fullerene substituent. As the results in Table (2) show, fullerene C<sub>60</sub> reaction is done by exothermic procarbazine, and energy is transferred from the system to the environment, as the values of  $\Delta H_{ad}$  are obtained for all the derivatives are negative. However, this phenomenon cannot have an effect on the reaction run, because, despite this increase, the enthalpy changes remain negative. Moreover, to examine the effect of temperature on fullerene substituent process, all thermodynamic parameters were calculated at the temperature range from 298.15 to 398.15 Kelvin in the 3°-3° range and the values were reported. As is seen in Table (2), the temperature of the enthalpy changes gradually increases with increasing temperature. Thus, the process of forming the desired compounds becomes warmer with increasing temperature, and the optimum temperature for the surface adsorption of all derivatives is 298 Kelvin [21].

#### Thermodynamic parameters

The adsorption enthalpy changes ( $\Delta H_{ad}$ ), and Gibbs free energy variations ( $\Delta G_{ad}$ ) were calculated *via* equations 3 and 4 respectively. In equation 3, H represents the sum of the thermal enthalpy and total energy and in the 4<sup>th</sup> equation, G stands for the sum of the thermal Gibbs free energy and total.

$$\Delta H_{ad} = H_{\text{procarbazine-C60}} - (H_{\text{procarbazine}} + H_{\text{C60}}) \quad (3)$$

$$\Delta G_{ad} = G_{\text{procarbazine-C60}} - (G_{\text{procarbazine}} + G_{\text{C60}}) \quad (4)$$

The obtained adsorption enthalpy changes and Gibbs free energy alterations are presented in Tables 2, 3. As it can be perceived from the results, the procarbazine adsorption on the surface of the fullerene (C<sub>60</sub>) is exothermic and spontaneous in all derivatives. But on the Other hand, the adsorption of this amino acid on the fullerene surface is endothermic and non-spontaneous at both configurations. The effect of temperature on the thermodynamic factors was also investigated. As it is obvious from the presented data, increasing of temperature does not have a remarkable effect on the values of enthalpy changes and Gibbs free energy alterations. Hence, it seems the ambient temperature is the best one for the procarbazine adsorption process. Procarbazine is the most widely used anticancer drug that to treat cancer. However, today its use is restricted as it produces toxic compounds. Thus, in this study, the effect of the substituent of fullerene C<sub>60</sub> and structural properties of procarbazine were studied. The thermodynamic parameters showed that the procarbazine drug reaction with fullerene C<sub>60</sub> is exothermic, spontaneous, and one-way and non-equilibrium and this reaction has the highest efficiency at room temperature [22].

**Table 1.** Total energy values , the lowest observed frequency, bond distances, bond type, zero-point energy, surface, for procarbazine and its derivatives with fullerene C<sub>60</sub>  
In the gas phase <sup>(a)</sup> and the water solvent phase <sup>(b)</sup>

		Procarbazine	I-Isomer	II-Isomer	III-Isomer
$\Delta E_{ad}$	a	-	-794.22	-828.83	-861.97
	b		-753.75	-720.62	-686.01
Lowest frequency (cm <sup>-1</sup> )	a	20.5806	9.9669	9.8476	6.3083
	b	16.7771	8.8313	6.6429	7.2518
N <sub>13</sub> -C <sub>35</sub> (Å)	a	-	1.52048	-	-
	b		1.52121		
N <sub>28</sub> -C <sub>35</sub> (Å)	a	-	-	1.51216	-
	b			1.51445	
N <sub>30</sub> -C <sub>35</sub> (Å)	a	-	-	-	1.51773
	b				1.51346

<sup>a</sup>value of vacuum, <sup>b</sup> value of solvent

As the results in Table (2) show, fullerene C<sub>60</sub> reaction is done by exothermic procarbazine, and energy is transferred from the system to the environment, as the values of  $\Delta H_{ad}$  are obtained for all the derivatives are negative. However, this phenomenon cannot have an effect on the reaction run, because, despite this increase, the enthalpy changes remain negative. Moreover, to examine the effect of temperature on fullerene substituent process, all thermodynamic parameters

were calculated at the temperature range from 298.15 to 398.15 Kelvin in the 3°-3° range and the values were reported. As is seen in Table (2), the temperature of the enthalpy changes gradually increases with increasing temperature. Thus, the process of forming the desired compounds becomes warmer with increasing temperature, and the optimum temperature for the surface adsorption of all derivatives is 298 Kelvin [23,24].

**Table 2.** The values of enthalpy variations in the formation of substituent reaction of fullerene C<sub>60</sub> and procarbazine in the gas phase (<sup>a</sup>) and the water solvent phase (<sup>b</sup>) at the temperature range from 278.15 to 314.15 Kelvin

Temperature(K)		$\Delta H_{ad}(KJ/mol)$		
		I-Isomer	II-Isomer	III-Isomer
278.15	a	-778.82	-814.08	-847.08
	b	-671.27	-706.52	-739.52
281.15	a	-778.83	-814.08	-847.07
	b	-671.27	-706.53	-739.52
284.15	a	-778.83	-814.08	-847.08
	b	-671.28	-706.53	-739.52
287.15	a	-778.83	-814.08	-847.08
	b	-671.28	-706.52	-739.52
290.15	a	-778.83	-814.08	-847.08
	b	-671.28	-706.52	-739.52
293.15	a	-778.84	-814.08	-847.08
	b	-671.28	-706.52	-739.52
296.15	a	-778.84	-814.08	-847.08
	b	-671.29	-706.52	-739.53
299.15	a	-778.84	-814.07	-847.08
	b	-671.29	-706.52	-739.53
302.15	a	-778.84	-814.07	-847.08
	b	-671.29	-706.52	-739.53
305.15	a	-778.85	-814.07	-847.08
	b	-671.30	-706.52	-739.54
308.15	a	-778.85	-814.06	-847.08
	b	-671.30	-706.51	-739.54

311.15	a	-778.85	-814.06	-847.08
	b	-671.30	-706.51	-739.54
314.15	a	-778.85	-814.06	-847.08
	b	-671.31	-706.51	-739.54

<sup>a</sup>value of vacuum, <sup>b</sup>value of solvent

**Table 3.** Gibbs free energy change of fullerene C<sub>60</sub> and procarbazine in the gas phase (<sup>a</sup>) and the water solvent phase (<sup>b</sup>) at the temperature range from 278.15 to 314.15 Kelvin

Temperature(K)		$\Delta G_{ad}(KJ/mol)$		
		I-Isomer	II-Isomer	III-Isomer
278.15	a	-710.11	-745.53	-778.92
	b	-602.69	-638.12	-671.51
281.15	a	-709.86	-745.30	-778.67
	b	-602.45	-637.89	-671.27
284.15	a	-709.61	-745.06	-778.43
	b	-602.20	-637.65	-671.02
287.15	a	-709.37	-744.82	-778.18
	b	-601.96	-637.41	-670.77
290.15	a	-709.12	-744.58	-777.94
	b	-601.71	-637.17	-670.53
293.15	a	-708.87	-744.34	-777.69
	b	-601.46	-636.94	-670.28
296.15	a	-708.62	-744.10	-777.44
	b	-601.22	-636.70	-670.04
299.15	a	-708.38	-743.86	-777.20
	b	-600.97	-636.46	-669.80
302.15	a	-708.13	-743.62	-776.95
	b	-600.73	-636.22	-669.56
305.15	a	-707.88	-743.37	-776.71
	b	-600.48	-635.98	-669.31
308.15	a	-707.63	-743.12	-776.46
	b	-600.24	-635.73	-669.07
311.15	a	-707.38	-742.87	-776.22
	b	-599.99	-635.48	-668.82
314.15	a	-707.13	-742.63	-775.97
	b	-599.73	-635.23	-668.57

<sup>a</sup>value of vacuum, <sup>b</sup>value of solvent

Procarbazine is the most widely used anticancer drug that to treat cancer. However, today its use is restricted as it produces toxic compounds. Thus, in this study, the effect of the substituent of fullerene C<sub>60</sub> and structural properties of procarbazine were studied. The

thermodynamic parameters showed that the procarbazine drug reaction with fullerene C<sub>60</sub> is exothermic, spontaneous, and one-way and non-equilibrium and this reaction has the highest efficiency at room temperature [25-27].

**Table 4.** The values of thermodynamic equilibrium constants for the for the procarbazine adsorption process with fullerene C<sub>60</sub> in the gas phase (<sup>a</sup>) and the water solvent phase (<sup>b</sup>) at the temperature range from 278.15 to 314.15 Kelvin

Temperature(K)		K <sub>th</sub>		
		I-Isomer	II-Isomer	III-Isomer
278.15	a	2.58×10 <sup>+124</sup>	4.15×10 <sup>+130</sup>	2.94×10 <sup>+136</sup>



	b	$3.92 \times 10^{+105}$	$6.30 \times 10^{+111}$	$4.47 \times 10^{+117}$
281.15	a	$8.98 \times 10^{+123}$	$1.38 \times 10^{+130}$	$9.32 \times 10^{+135}$
	b	$1.58 \times 10^{+105}$	$2.43 \times 10^{+111}$	$1.64 \times 10^{+117}$
284.15	a	$3.14 \times 10^{+123}$	$4.64 \times 10^{+129}$	$2.97 \times 10^{+135}$
	b	$6.37 \times 10^{+104}$	$9.41 \times 10^{+110}$	$6.03 \times 10^{+116}$
287.15	a	$1.11 \times 10^{+123}$	$1.56 \times 10^{+129}$	$9.57 \times 10^{+134}$
	b	$2.59 \times 10^{+104}$	$3.66 \times 10^{+110}$	$2.24 \times 10^{+116}$
290.15	a	$3.93 \times 10^{+122}$	$5.31 \times 10^{+128}$	$3.10 \times 10^{+134}$
	b	$1.06 \times 10^{+104}$	$1.43 \times 10^{+110}$	$8.37 \times 10^{+115}$
293.15	a	$1.40 \times 10^{+122}$	$1.82 \times 10^{+128}$	$1.01 \times 10^{+134}$
	b	$4.36 \times 10^{+103}$	$5.65 \times 10^{+109}$	$3.15 \times 10^{+115}$
296.15	a	$5.05 \times 10^{+121}$	$6.26 \times 10^{+127}$	$3.33 \times 10^{+133}$
	b	$1.80 \times 10^{+103}$	$2.24 \times 10^{+109}$	$1.19 \times 10^{+115}$
299.15	a	$1.83 \times 10^{+121}$	$2.17 \times 10^{+127}$	$1.11 \times 10^{+133}$
	b	$7.52 \times 10^{+102}$	$8.93 \times 10^{+108}$	$4.55 \times 10^{+114}$
302.15	a	$6.66 \times 10^{+120}$	$7.57 \times 10^{+126}$	$3.69 \times 10^{+132}$
	b	$3.15 \times 10^{+102}$	$3.587 \times 10^{+108}$	$1.75 \times 10^{+114}$
305.15	a	$2.44 \times 10^{+120}$	$2.66 \times 10^{+126}$	$1.24 \times 10^{+132}$
	b	$1.33 \times 10^{+102}$	$1.44 \times 10^{+108}$	$6.74 \times 10^{+113}$
308.15	a	$9.02 \times 10^{+119}$	$9.37 \times 10^{+125}$	$4.20 \times 10^{+131}$
	b	$5.62 \times 10^{+101}$	$5.84 \times 10^{+107}$	$2.62 \times 10^{+113}$
311.15	a	$3.35 \times 10^{+119}$	$3.33 \times 10^{+125}$	$1.43 \times 10^{+131}$
	b	$2.39 \times 10^{+101}$	$2.38 \times 10^{+107}$	$1.02 \times 10^{+113}$
314.15	a	$1.25 \times 10^{+119}$	$1.19 \times 10^{+125}$	$4.92 \times 10^{+130}$
	b	$1.02 \times 10^{+101}$	$9.73 \times 10^{+106}$	$4.01 \times 10^{+112}$

**Table 5.** Calculated  $E_H$  and  $E_L$ , band gap (HLG), chemical hardness ( $\eta$ ), electrophilicity index ( $\omega$ ), the maximum amount of electronic charge index ( $\Delta N_{max}$ ) and dipole moment for the procarbazine adsorption process in the gas(a) and water solvent(b) phase

	$E_H$ (eV)	$E_L$ (eV)	HLG (eV)	$\eta$ (eV)	$\mu$ (eV)	$\omega$ (eV)	$\Delta N_{max}$ (eV)	Dipole Moment(Deby)
procarbazine	-7.42 <sup>a</sup>	6.10	13.52	6.76	-0.66	-34.62	0.10	3.34
	-7.29 <sup>b</sup>	6.21	13.50	6.75	-0.54	-42.19	0.08	3.59
I-Isomer	-5.25 <sup>a</sup>	3.07	8.32	4.16	-1.09	-7.94	0.26	3.04
	-5.63 <sup>b</sup>	3.79	9.42	4.71	-0.92	-12.06	0.20	4.75
II-Isomer	-5.39 <sup>a</sup>	2.94	8.33	4.17	-1.23	-7.08	0.29	2.91
	-5.21 <sup>b</sup>	2.25	7.88	3.94	-1.69	-4.59	0.43	7.05
III-Isomer	-5.27 <sup>a</sup>	3.06	8.33	4.17	-1.11	-7.85	0.27	2.51
	-5.64 <sup>b</sup>	3.80	9.44	4.72	-0.92	-12.11	0.19	1.70

### Conclusion

The bipolar state of the studied structures has also been studied. This parameter is a good criterion for evaluating the solubility of molecules in polar solvents. Molecules with higher dipole moments have better solubility in water and compounds with less bipolar moments will be weaker in polar solvents. As can be seen, the dipole moment of procarbazine decreases after fullerene connection. Thus, carbon

nanotube derivatives with procarbazine have less solubility in water compared to pure procarbazine. Procarbazine determination is of a great importance in medical and nutritional fields. In this regard, the performance of fullerene ( $C_{60}$ ) as a sensing material in the thermal and electrochemical biosensors was investigated by density functional theory. The obtained results exhibit that procarbazine adsorption on the surface of the fullerene ( $C_{60}$ ) is exothermic,



spontaneous, non-equilibrium and experimentally feasible. However, the adsorption of procarbazine on the fullerene surface is endothermic, non-spontaneous, equilibrium, and experimentally impossible. The calculated band gap, electrophilicity and specific heat capacity parameters show that fullerene (C<sub>60</sub>) can act as an excellent electroactive and thermal sensing material in the construction of procarbazine potentiometric, conductometric and thermal sensors. In this regard, the experimental use of this nanostructure in the detection of procarbazine is recommended to be evaluated by the experts of this field.

#### Acknowledgements

The author appreciates the Islamic Azad University of Tehran North Branch Research Council for the support of this project.

#### References

- [1] L. Szabos, A. Savoure, *Trends. Plant. SCI.*, **2010**, *15*, 89-97.
- [2] L.K. Liu, D.F. Becker, J.J. Tanner, *Arc. Biochem. Biophys.*, **2017**, *632*, 147-157.
- [3] M.M. Gomez, R. Motila, E. Diez, *Electrochim. Acta.*, **1989**, *34*, 831-839.
- [4] L.G. Heller, E.R. Kirch, *J. Am. Pharm. Assoc.*, **1947**, *36*, 345-349.
- [5] P. Chang, Z. Zhang, C. Yang, *Anal. Chim. Acta.*, **2010**, *666*, 70-75.
- [6] J.W. Costin, N.W. Barnett, S.W. Lewis, *Talanta.*, **2004**, *64*, 894-898.
- [7] H. Zheng, Y. Hirose, T. Kimura, S. Suye, T. Hori, H. Katayama, J. Arai, R. Kawakami, T. Ohshima, *Sci. Tech. Adv. Mater.*, **2006**, *7*, 243-248.
- [8] C. Truzzi, A. Annibaldi, S. Illuminati, C. Finale, G. Scarponi, *Food. Chem.*, **2014**, *150*, 477-481.
- [9] M. Nabati, M.S. Kermanian, H. Mohammadnejad-Mehrabani, H. Rahbar Kafshboran, M. Mehmannaavaz, S. Sarshar, *Chemical Methodologies.*, **2018**, *2*, 128-140.
- [10] A. Bahrami, S. Seidi, T. Baheri, M. Aghamohammadi, *Superlattices. Microstruct.*, **2013**, *64*, 265-273.
- [11] M.D. Esrafil, *Phys. Lett.*, **2017**, *381*, 2085-2091.
- [12] A. Vinu, T. Mori, K. Ariga, *Sci. Technol. Adv. Mater.*, **2006**, *7*, 753-771.
- [13] A. Soltani, M.T. Baei, M. Mirarab, M. Sheikhi, E.T. Lemeskhi, *J. Phys. Chem. Solids.*, **2014**, *75*, 1099-1105.
- [14] S.A. Siadati, M.S. Amini-Fazl, E. Babanezhad, *Sens. Actuators. B. Chem.*, **2016**, *237*, 591-596.
- [15] R. Rahimi, S. Kamalinahad, M. Solimannejad, *Mater. Res. Express.*, **2018**, *5*, 1-17.
- [16] P. Pakravan, S.A. Siadati, *J. Mol. Graph. Model.*, **2017**, *75*, 80-84.
- [17] M.T. Baei, *Heteroatom. Chem.*, **2013**, *24*, 516-523.
- [18] M. Soleymani, H.D. Khavidaki, *Comput. Theor. Chem.*, **2017**, *1112*, 37-45.
- [19] R. Ahmadi, M.R. Jalali Sarvestani, *Phys. Chem. Res.*, **2018**, *6*, 639-655.
- [20] M.R. Jalali Sarvestani, R. Ahmadi, *Int. J. New. Chem.*, **2018**, *4*, 400-408.
- [21] M.R. Jalali Sarvestani, R. Ahmadi, *Int. J. New. Chem.*, **2018**, *5*, 409-418.
- [22] R. Ahmadi, M.R. Jalali Sarvestani, *Int. J. Bio-Inorg. Hybrid. Nanomater.*, **2017**, *6*, 239-244.
- [23] R. Ahmadi, *Int. J. Nano. Dimens.*, **2017**, *8*, 250-256.
- [24] M.R. Jalali Sarvestani, L. Hajiaghbabaei, J. Najafpour, S. Suzangarzadeh, *Anal. Bioanal. Electrochem.*, **2018**, *10*, 675-698.
- [25] W. Schnelle, R. Fischer, J. Gmelin, *J. Phys. D. Appl. Phys.*, **2001**, *34*, 846-851.
- [26] Z. Javanshir, S. Jameh-Bozorgh, P. Peyki, *Adv. J. Chem. A.*, **2018**, *1*, 117-126.

[27] R. Ahmadi, M.R. Jalali Sarvestani, *Iranian Chemical Communication*, **2019**, 7, 344-351.

**How to cite this manuscript:** Behnam Farhang Rik, Roya Ranjineh khojasteh, Roya Ahmadi, Maryam Karegar Razi. "Evaluation of C60 nano-structure performance as nano-carriers of procarbazine anti-cancer drug using density functional theory methods". *Eurasian Chemical Communications*, 2019, 359-368.